

# Numerical Analysis of an Ethanol-Water Distillation System using Computational Fluid Dynamics (CFD)

Taedong Kim<sup>1)</sup> and Taewon Seo<sup>2)</sup>

**Abstract**— The purposes of this study are to predict the amount of alcohol produced per day, and to investigate the flow characteristics for given geometry and operating conditions. The parameters examined in this study are both the operating temperature, and the vacuum pressure at the outlet-top region. Velocity profiles and distribution of volume fraction were calculated in the distillation column model using CFD (Computational Fluid Dynamics). The efficiency in order to obtain more than vapor from the mixture will increase if the operating temperature sets up high under the constant vacuum pressure. It can be seen that the distribution profiles of vapor volume fraction as well as the magnitude of volume fraction appears quite different at  $T=45^{\circ}\text{C}$ .

**Index Term**— Distillation column; CFD; Volume fraction; Multiphase flow; Separation process

## I. INTRODUCTION

Distillation is one of the most important separation processes in chemical and petroleum industries [1,4,9], mainly because it allows separating ideal and non-ideal mixtures in large-scale units. The separation of homogeneous and heterogeneous azeotropic mixtures is of great industrial interest, and a large number of such distillation columns are in operation. Furthermore, the necessity in developing new feasible sequences of distillation columns has increased, in order to attend demands of clean and economical processes [2,10].

Distillation is a method for separating two or more liquid compounds on the basis of boiling-point differences [3,7,9]. The boiling point of a mixture is a function of the vapor pressures of the various components in the liquid mixture. As a liquid is heated, its kinetic energy increases; more molecules move into the gaseous state, thereby increasing the vapor pressure. Therefore, the prediction on column efficiency to separate the ethanol from the mixtures relies on the fact that mass and heat transfer between the liquid and vapor phases [6,9,10].

There are considerable interests in the use of CFD to model the separation technique in some chemical equipment [4,5]. The multiphase models that can apply in the distillation column are volume of fluid (VOF), mixture and Eulerian models. The VOF model can be applied to simulate the multiphase flow for

gas-liquid flow [6,7,8,11]. Singh [9] studied a design and prediction of concentration and temperature distribution for Benzene-Toluene system using two-phase Eulerian framework. In this study a mixture model was developed to give the predictions of the amount of alcohol produced per day.

There is little known about the flow behavior and mass- and heat-transfer due to the complex behaviors of the multiphase flow in the distillation column. A better understanding of the flow characteristics during the separation process is able to determine the optimal equipment design. Thus, the objectives of the study are to predict the amount of alcohol produced per day, and to investigate the flow characteristics for given geometry and operating conditions.

## II. FORMULATION OF PROBLEMS

### A. Problem Description

The multicomponent distillation columns were modelled using the multiphase flow CFD. The model considers the flows of vapor and liquid phases in the mixture model in the liquid mixture. Fig. 1 shows the real distillation equipment constructed in the factory to extract the alcohol. The problem to be solved in the study is shown in Fig. 2. The diameter of the pipe line in the equipment is 23mm. The diameter of distillation column is  $D$ , 270 mm and the height of the column is 3,000 mm. In Fig. 1, the 11 baffles are installed in the distillation column and the diameter of baffle is  $2D/3$  and the thickness is 2 mm. The Distillation columns are made up of several components, each of which is used either to transfer heat energy or enhance material transfer. The geometry of distillation column is designed by using ANSYS Workbench 14.5 and then it is inputted onto FLUENT for simulation alcohol distillation.

The mixture flowing into the distillation column at room temperature is composed of water and liquid alcohol. The flow rate of the mixture is 600L/hr. The amount of alcohol contained in the mixture is about 156~164L, while the rest is water. During the separation process, the distillation system was designed that 95% of the amount of alcohol contained in the mixture is to be evaporated into the top outlet. However, we assumed that 5% of the alcohol did not change the phase from liquid to vapor in the distillation column and falls down to the bottom outlet. The mechanical properties of ethanol and water compound are shown in Table II.

- 1) T.D Kim is with the Andong National University, Andong, 760-749 Korea
- 2) T.W Seo is with the Andong National University, Andong, 760-749 Korea (Corresponding Author, phone: 82-54-820-5756; fax: 82-54-820-5044; e-mail: [dongjin@anu.ac.kr](mailto:dongjin@anu.ac.kr))

Table II  
Mechanical properties of ethanol and water compound

Compound	Ethanol	Water
Boiling Point( °C)	78.5	100
Density (g/mL)	0.789	1.00
Viscosity (Pa*s)	0.001095	0.001002
Specific Heat C <sub>p</sub> (J/kg K)	2,720	4,182
Thermal Conductivity (W/mK)	0.171	0.598
Thermal Expansion (K <sup>-1</sup> )	1,120X10 <sup>-06</sup>	0.207X10 <sup>-03</sup>

### B. Governing Equations, Boundary Conditions and Solution Method

The mixture model using ANSYS FLUENT v14.5 is applied for the study. The mixture model can model water and ethanol by solving the continuity, momentum and energy equations for the mixture and the volume fraction equations for the secondary phases, which indicate the ethanol.

The continuity equation for the mixture is [11]:

$$\frac{\partial \rho_m}{\partial t} + \nabla \cdot (\rho_m \vec{v}_m) = 0 \quad (1)$$

where  $\vec{v}_m$  is the mass-averaged velocity and  $\rho_m$  is the mixture density.

$$\begin{aligned} \vec{v}_m &= \frac{\sum_{i=1}^2 \alpha_i \rho_i \vec{v}_i}{\rho_m} \\ \rho_m &= \sum_{i=1}^2 \alpha_i \rho_i \end{aligned} \quad (2)$$

where  $\alpha_i$  is the volume fraction of phase i.

The momentum equation for the mixture can be obtained by summing the individual momentum equations for all phases:

$$\begin{aligned} \frac{\partial \vec{v}_m}{\partial t} + \nabla \cdot (\vec{v}_m \vec{v}_m) &= -\frac{1}{\rho_m} \nabla p + \nabla \cdot [v_m (\nabla \vec{v}_m)] + \rho_m \vec{g} \\ + \nabla \cdot (\sum_{i=1}^2 \alpha_i \rho_i \vec{u}_{dr,i}^2) \end{aligned} \quad (3)$$

where  $v_m$  is the fluid kinematic viscosity of the mixture,  $\vec{u}_{dr,i} = \vec{v}_i - \vec{v}_m$  is the drift velocity vector for the secondary phase i, and  $\rho_i$  is the fluid density for the secondary phase i.

The energy equation for i<sup>th</sup> phase takes the following form:

$$\frac{\partial}{\partial t} (\alpha_i \rho_i E_i) + \nabla \cdot [\alpha_i \vec{v}_i (\rho_i E_i + p)] = \nabla \cdot (K \nabla T) \quad (4)$$

where K is the conductivity.

From the continuity equation for secondary phase p, the volume fraction equation can be obtained:

$$\begin{aligned} \frac{\partial}{\partial t} (\alpha_p \rho_p) + \nabla \cdot (\alpha_p \rho_p \vec{v}_m) &= \\ -\nabla \cdot (\alpha_p \rho_p \vec{v}_{dr,p}) + \sum_{q=1}^2 (\dot{m}_{qp} - \dot{m}_{pq}) \end{aligned} \quad (5)$$

The relative velocity is defined as the velocity of a secondary phase (p) relative to the velocity of the primary phase (q):

$$\vec{v}_{pq} = \vec{v}_p - \vec{v}_q \quad (6)$$

The mass fraction for any phase (i) is defined as

$$c_i = \frac{\alpha_i \rho_i}{\rho_m} \quad (7)$$

The drift velocity and the relative velocity are connected by the following expression:

$$\vec{v}_{dr,p} = \vec{v}_{pq} - \sum_{i=1}^2 c_i \vec{v}_{qi} \quad (8)$$

Following Manninen et al [3], the relative velocity is given by

$$\vec{v}_{pq} = \frac{\tau_p (\rho_p - \rho_m)}{f_{drag} \rho_p} \vec{a} \quad (9)$$

where  $\tau_p$  is the particle relaxation time,  $\tau_p = \frac{\rho_p d_p^2}{18 \mu_p}$ .  $d$  is the diameter of the droplets of secondary phase p,  $\vec{a}$  is the secondary phase droplet's acceleration. The drag function in turbulent flow is given by  $f_{drag} = 0.0183 \text{Re}$  and the acceleration is of the flow

$$\vec{a} = \vec{g} - (\vec{v}_m \cdot \nabla) \vec{v}_m - \frac{\partial \vec{v}_m}{\partial t} \quad (10)$$

The mixture was assumed to flow in the distillation column and gas extracted from the liquid ethanol was assumed to exit through the outlet-top at the inlet as shown in Fig. 2. At the inlet, uniform velocity of the mixture,  $v=0.207$  m/s, is imposed and no-slip condition on the wall for both phases was applied for the two phases. The pressure conditions at the outlet-top and outlet-bottom region were also applied. The pressure at the outlet-top was given either -0.08 or -0.09MPa using the vacuum pump in Fig. 1c. The temperature at the outlet was set up one temperature in 40 or 45°C at the control panel in Fig. 1b.

The governing equations were solved using the commercial computational fluid dynamic code FLUENT (ANSYS v14.5, Pittsburgh, USA). In the simulation, the primary phase was set up water, while the secondary phase was liquid alcohol and the third phase was vapor alcohol. To simulate the phase change from the liquid alcohol to vaporize, evaporation-condensation model was applied. The QUICK scheme for momentum equations and volume fraction are applied implicitly for spatial discretization. The power law method was applied to turbulent kinetic energy equation and the second upwind method for turbulent dissipation rate. The SIMPLEC algorithm was applied to calculate pressure-velocity coupling scheme. Unstructured meshes with tetrahedral cells were used in all simulations. For the mesh sensitivity simulations, the meshes ranged from 44,449 to 2,166,280 and finally choose the 1,585,394 meshes for simulations.

All simulations were performed using a 2.8 GHz Windows 7 (32 GB of RAM, 64 bit) personal computer. The time increment used in here is 0.1 second. During the simulation the volume fraction of the vapor phase is investigated and steady state is reached in approximately 35 seconds from the start of the system. In simulations, convergence for each time step was based on the residual in continuity falling below a prescribed value (typically  $10^{-5}$ ). All solutions presented have been

verified to be mesh-independent – increasing the mesh density yields velocities that are within 1% of those shown here and flow separation zone lengths that are within 5% of those given.

### III. RESULTS AND DISCUSSION

The working fluid as a mixture is composed of water and alcohol. In the simulation water is a primary phase and alcohol is used as the gas and liquid phases. Fig. 3 indicates the lines and planes to provide the flow characteristics to discuss the results in this study. The initial stage after the distillation system operates is the unsteady state. However, after 35 seconds the distillation system operates, the system becomes the steady state. Here we present the results for the distillation system before reaching the steady state condition. Therefore, after 35 seconds the flow characteristics are not dependent on the time.

#### A. Flow Characteristics in the Distillation Column

Fig. 4 illustrates the velocity contours of mixture in the symmetry plane of the distillation column before the flow reaches the steady state. The temperature sets up at 40°C and pressure at the outlet-top fixed at  $P=-0.08\text{MPa}$ . After the system unit worked, the results showed for  $t=27, 33$  and  $35$  seconds, respectively.

The velocity is higher to the top plate in the outlet-top region due to the more vapor composition as time increases. The lower velocities in the middle regions among the plates are shown in Fig. 4. It is that the lighter gas is accumulated near the plate, while the heavier liquid is stagnant in the middle region. It is noticed the existence of circulation zones near the plate and the liquid caused to be falling to the outlet-bottom.

Fig. 5 presents the volume fractions for liquid (Fig. 5a, b, c) and vapor (Fig. 5d, e, f) distributions in the symmetry plane of the distillation column. At the beginning of the operation of the unit (see Fig. 5a and d), the whole region of the distillation column is filled by the mixture liquid. As operating time increases, the mixture can change the phase as can see in Fig. 5b and e. As a result, the more gas is extracted from the mixture. In addition the gas is lighter than the liquid, the gas flows toward the outlet-top and the liquid drops downward the outlet-bottom. It is also noted that the liquid and vapor phase distributions have a less homogenous.

The distribution profile of the vapor volume fraction at the indicated heights (L1, L2, L4 and L5) are shown in Fig. 6 for  $P=-0.08$  and  $-0.09\text{MPa}$  at  $T=40$  and  $45^\circ\text{C}$ . Even the magnitudes of the volume fractions differ for the different pressure conditions, the volume fraction patterns are similar as shown in Fig. 6a and b. As the mixture flows toward the top of the column, the liquid molecules are changing the phase into the vapor. Thus the mass fraction of gas in vapor phase is increasing and that in liquid phase is decreasing in the top region of the distillation column. The vapor elevation is more pronounced in the outlet-top region.

#### B. Effects of the Temperature and Pressure in Distillation Column

In this section it can be discussed the effects of the

temperature and pressure in the distillation column. Fig. 7 illustrates the behavior of liquid and vapor volume fractions for two different temperatures  $T=40$  and  $45^\circ\text{C}$  at a constant pressure  $P=-0.08\text{MPa}$ . It is well known that a liquid in a vacuum has a lower boiling point than when that liquid is at atmospheric pressure. Fig. 7 confirms that the phase change from the liquid to vapor in the mixture composition is quicker at the higher temperature. As a liquid is heated, its kinetic energy increases; the equilibrium shifts to the right and more molecules move into the gaseous state, thereby increasing the vapor pressure.

Fig. 8 shows the vapor volume fraction plot at L1 and L5 locations. The L1 is positioned near the outlet-top region and the L5 is located near the outlet-bottom region. At the L1, the amount of vapor is approximately 42% higher at  $T=45^\circ\text{C}$  than at  $T=40^\circ\text{C}$ . It is observed in Fig. 8a and b that the distribution of the volume fraction of the vapor phase presents a great variation in the L5 region compared with in the L1 region. In Fig. 8 the distribution of vapor volume fraction at  $T=45^\circ\text{C}$  is much more homogeneous than the distribution at  $T=40^\circ\text{C}$ . As a result, the efficiency in order to obtain more than vapor from the mixture will increase if the operating temperature sets up high under the constant vacuum pressure.

Fig. 9 demonstrates the vapor contours at the indicated plane in Fig. 3 to investigate the effect of vacuum pressure variation. The results showed that the profile patterns are similar at each plane when compared the contours at  $P=-0.08\text{MPa}$  with  $P=-0.09\text{MPa}$ .

Fig. 10 presents the volume fraction at the L1 and L5 at  $T=40^\circ\text{C}$ . As seen in figure, the distribution profiles of vapor volume fraction has same pattern, while the magnitude of volume fraction is different. This confirmed the results shown in Fig. 9. Therefore, it may be concluded that the pressure variation is not expected to significantly affect the vapor volume fraction. However, the pressure is likely to affect the vapor volume fraction for temperature  $T=45^\circ\text{C}$  as shown in Fig. 11. It can be seen that the distribution profiles of vapor volume fraction as well as the magnitude of volume fraction appears quite different for temperature  $T=45^\circ\text{C}$  (see Fig. 11).

### IV. CONCLUSIONS

Our goal in developing this model was to examine the distillation column performance and to investigate the flow characteristics for a given geometry. Computer simulations were conducted to quantify the effect of operating temperatures as well as vacuum pressure as the outlet-top boundary condition. In this study the numerical investigation is performed to understand the flow characteristics in the distillation column under the two different temperatures  $T=40$  and  $45^\circ\text{C}$ . The results were compared in terms of the distribution of velocity and vapor volume fraction in the distillation column.

The main findings of this study can be summarized as follows:

1. The velocity is higher to the top plate in the distillation column and the heavier liquid in the lower velocity is stagnant in the middle region among the plates.

2. The mass fraction of gas in vapor phase is increasing and that in liquid phase is decreasing in the top region of the distillation column.
3. The efficiency in order to obtain more than vapor from the mixture will increase if the operating temperature sets up high under the constant vacuum pressure.
4. It can be seen that the distribution profiles of vapor volume fraction as well as the magnitude of volume fraction appears quite different at  $T=45^{\circ}\text{C}$ .

## REFERENCES

- [1] Bhatt, K. and Patel, N.M., Generalized modeling and simulation of reactive distillation: Esterification, *Adv. App. Sci. Res.*, 3 (2012), 1346-1352.
- [2] Li, W., Liu, B., Yu, G. and Yuan, X., A new model for the simulation of distillation column, *Chinese J. Chem. Eng.*, 19 (2011), 717-725.
- [3] Manninen, M., Taivassalo, V. and Kallio, S., On the mixture model for multiphase flow, *VTT Publications* 288, Technical Research Center of Finland, 1996.
- [4] Olafadehan, O.A., Adeniyi, V.O., Popoola, L.T. and Salami, L., Mathematical modelling and simulation of multicomponent distillation column for acetone-chloroform-methanol system, *Adv. Chem. Eng. Res.* 2 (2013), 113-123.
- [5] Owens, S.A., Perkins, M.R. and Eldridge, R.B., Computational fluid dynamics simulation of structured packing, *I & EC Res.*, 52 (2013), 2032-2045.
- [6] Pinto, R.T.P., Wolf-Maciel, M.R. and Lintomen, L., Saline extractive distillation process for ethanol purification, *Computers & Chemical Engineering*, 24 (2000): 1689-1694.
- [7] Pulido, J.L., Martinez, E.L., Bineli, A.R.R., Wolf, M.R. and Filho, R.M., Heat transfer study in a concentric stage of an internally heat-integrated distillation column (HIDiC) using CFD simulation, *Proceeding World Cong. Eng. And Computer Sci.*, Oct. 20-22 (2010), San Francisco, USA
- [8] Rahimi, M.R. and Karimi, H., Modeling distillation mass transfer efficiency, *Inter. J. Chem. And Environ. Eng.*, 2 (2011), 165-167.
- [9] Singh, S., CFD simulations of benzene-toluene system over sieve tray, *Inter. J. Eng. Sci. and Emerging Tech.* 3 (2012), 81-89.
- [10] Sun, Z.M., Yuan, X.G., Liu, C.J. and Yu, K.T., A modified model of computational mass transfer for distillation column, *Symposium series* 105 (2006), 282-293.
- [11] Teleken, J.G., Werle, L.O., Marangoni, C., Quadri, M.B. and Machado, R.A.F., CFD simulation of multiphase flow in a sieve tray of a distillation column, *Brazilian J. Petroleum and Gas*, 3 (2009), 1-12.

**Taewon Seo** received the PhD degree in Mechanical Engineering from Louisiana State University in 1993, Baton Rouge, LA, USA.

He worked at R & D center of Korea Heavy Industries Ltd. as the Senior Researcher from Feb. 1994 to Feb. 1996. He joined the Andong National University in March 1996. Prof. Seo visited the Department of Hydraulics of Tsinghua University, Beijing, China in Jan., 1998 and the Institute of Fluid mechanics at Erlangen University, Erlangen, Germany in June, 2001 as the visiting scholar. He had a sabbatical year in 2002 at Department of Aeronautical and Mechanical Engineering in University of California, Davis, USA. Previous research interests of Prof. Seo were the flow control and management as well as the two-phase particulate flows. The current research interest is the bio-fluid mechanics.

Prof. Seo works at the Department of Mechanical and Automotive Engineering in Andong National University, Korea. He is member of KSME and Korean Society of Rheology.

**Tae-Dong Kim** received the PhD degree in Biotechnology from Tokyo Institute of Technology in 1995, Tokyo, Japan. After he received PhD, he worked Research center of Ministry of Health, Labour and Welfare, Japan from April, 1995 to Feb., 1997. Then he joined at the Department of Environmental Engineering of the Andong National University in March 1997. Prof. Kim played an important role to provide the environmental policies for Ministry of Environment in Korea as an Environment adviser. He had a sabbatical year in 2010 at Department of Civil and Environmental Engineering in University of Delaware, USA. Research interests of Prof. Kim were the Nonpoint source pollution and management of waste materials.

Prof. Kim is member of Korean Society on Water Quality and Korean Society of Waste Management.

a) Distillation column equipment



b) Control panel



c) Schematic diagram of the equipment

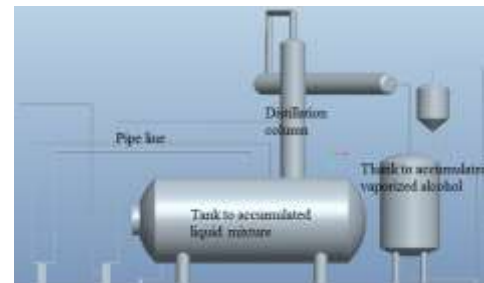
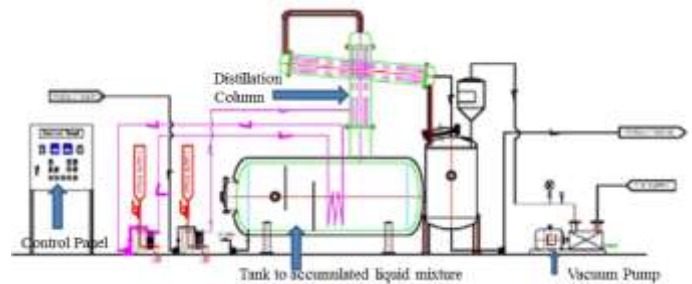


Fig. 1. Real distillation equipment constructed in the factory to extract the alcohol

a) Model geometry



b) Installed baffles inside the column



Fig. 2. Mathematical geometry for distillation column taken from Figure 1

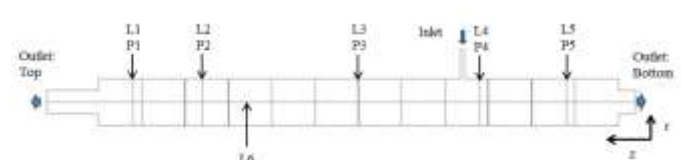


Fig. 3. Examined lines and planes in the symmetry plane of the distillation column

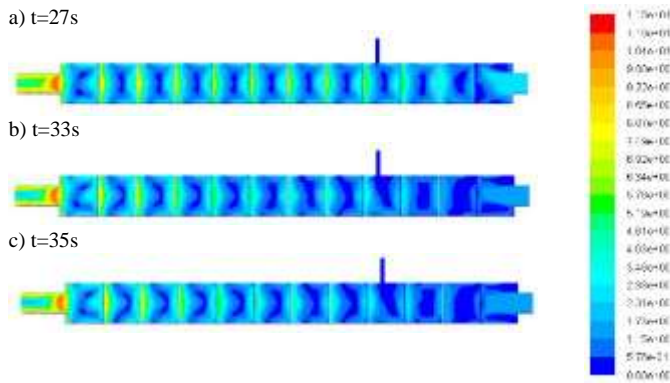


Fig. 4. Velocity contours in the symmetry plane of the distillation column

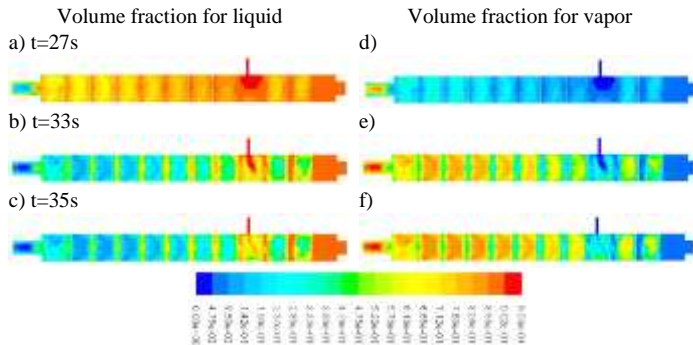
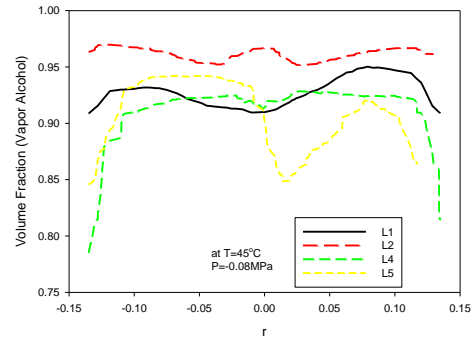


Fig. 5. Volume fraction of liquid and vapor in the symmetry plane of the distillation column



d)

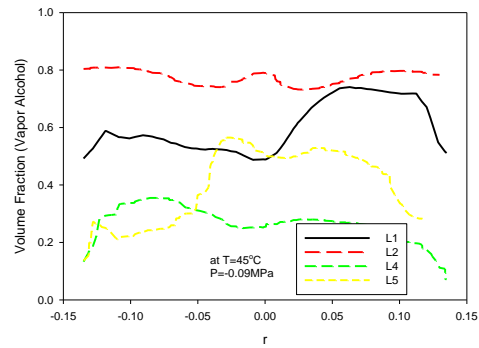
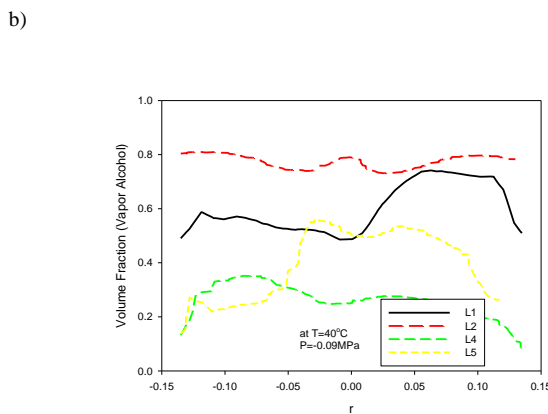
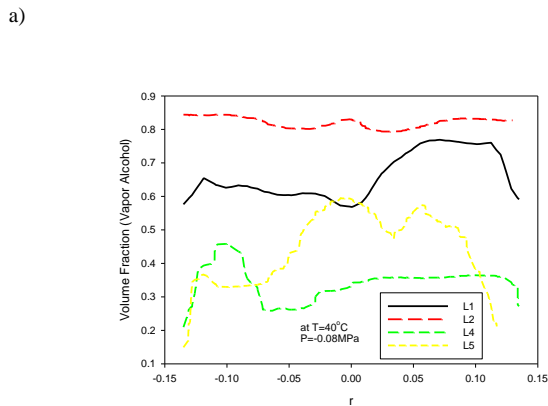


Fig. 6. Volume fraction of vapor alcohol at the given line of the distillation column



c)

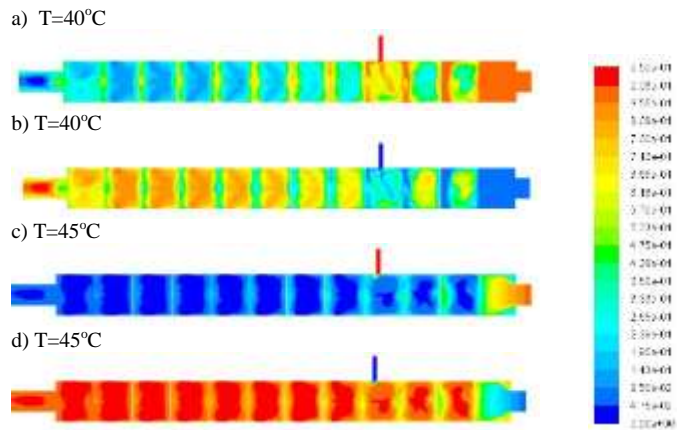
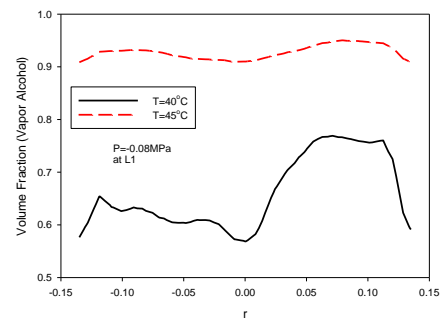


Fig. 7. Volume fraction of liquid and vapor alcohol at the symmetry plane of the distillation column at constant pressure P=0.08MPa

a) at L1



b) at L5

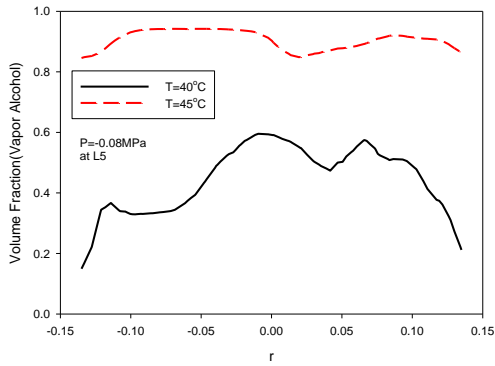
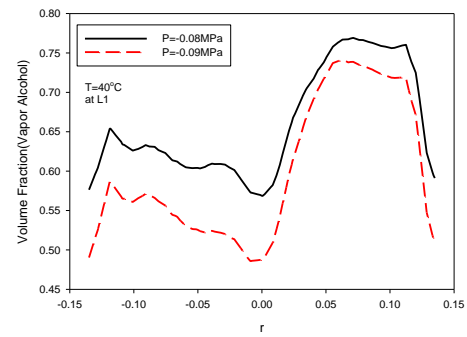


Fig. 8. Volume fraction of vapor alcohol at the L1 and L5 of the distillation column at constant pressure  $P=-0.08\text{MPa}$



b) at L5

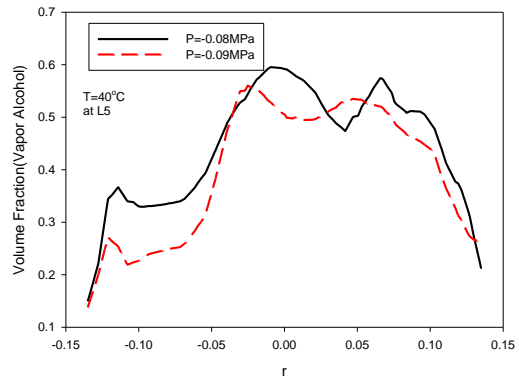
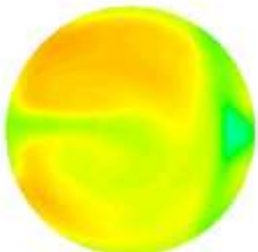
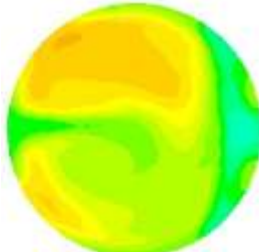


Fig. 10. Volume fraction of vapor alcohol at the L1 and L5 of the distillation column at constant temperature  $T=40^\circ\text{C}$

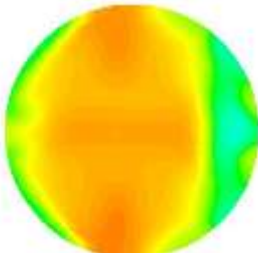
a)  $P=-0.08\text{MPa}$  at P1



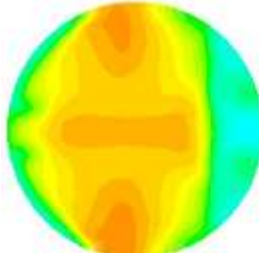
e)  $P=-0.09\text{MPa}$  at P1



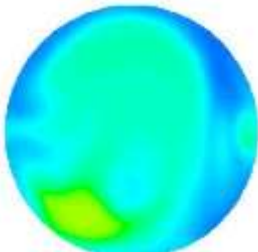
b)  $P=-0.08\text{MPa}$  at P2



f)  $P=-0.09\text{MPa}$  at P2



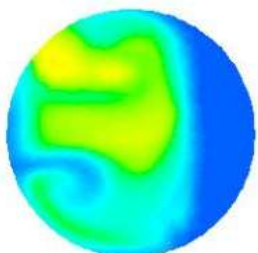
c)  $P=-0.08\text{MPa}$  at P4



g)  $P=-0.09\text{MPa}$  at P4



d)  $P=-0.08\text{MPa}$  at P5



h)  $P=-0.09\text{MPa}$  at P5

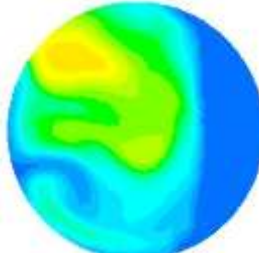
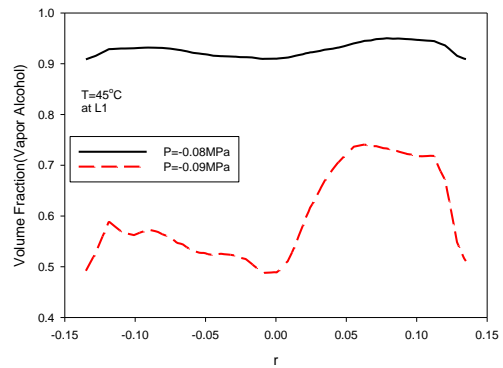


Fig. 9. Volume fraction of vapor alcohol at the indicated plane of the distillation column for constant temperature  $T=40^\circ\text{C}$

a) at L1



b) at L5

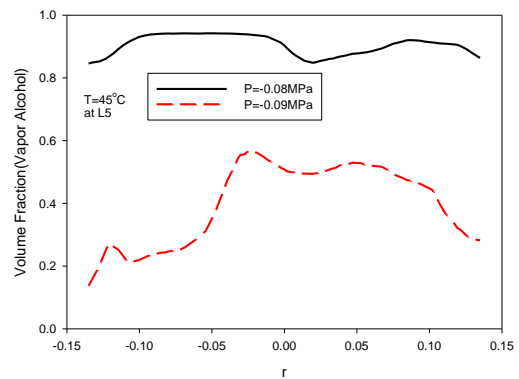


Fig. 11. Volume fraction of vapor alcohol at the L1 and L5 of the distillation column at constant temperature  $T=45^\circ\text{C}$

a) at L1